

PyDaddy: A Python package for discovering stochastic dynamical equations from timeseries data

Arshed Nabeel,^{1,*} Ashwin Karichannavar,^{1,*} Shuaib Palathingal,¹
Jitesh Jhawar,^{2,3} Danny Raj M.,⁴ and Vishwesh Guttal¹

¹Center for Ecological Sciences,
Indian Institute of Science, Bengaluru

²University of Konstanz, Konstanz, Germany

³Max Planck Institute of Animal Behaviour, Konstanz, Germany

⁴Department of Chemical Engineering,
Indian Institute of Science, Bengaluru

(Dated: May 6, 2022)

Most real-world ecological dynamics, ranging from ecosystem dynamics to collective animal movement, are inherently stochastic in nature. *Stochastic differential equations* (SDEs) are a popular modelling framework to model dynamics with intrinsic randomness. Here, we focus on the inverse question: If one has empirically measured time-series data from some system of interest, is it possible to discover the SDE model that best describes the data. Here, we present PyDaddy (Python library for **Data Driven Dynamics**), a toolbox to construct and analyze interpretable SDE models based on time-series data. We combine traditional approaches for data-driven SDE reconstruction with an *equation learning* approach, to derive symbolic equations governing the stochastic dynamics. The toolkit is presented as an open-source *Python* library, and consists of tools to construct and analyze SDEs. Functionality is included for visual examination of the stochastic structure of the data, guided extraction of the functional form of the SDE, and diagnosis and debugging of the underlying assumptions and the extracted model. Using simulated time-series datasets, exhibiting a wide range of dynamics, we show that PyDaddy is able to correctly identify underlying SDE models. We demonstrate the applicability of the toolkit to real-world data using a previously published movement data of a fish school. Starting from the time-series of the observed polarization of the school, pyDaddy readily discovers the SDE model governing the dynamics of group polarization. The model recovered by PyDaddy is consistent with the previous study. In summary, stochastic and noise-induced effects are central to the dynamics of many biological systems. In this context, we present an easy-to-use package to reconstruct SDEs from timeseries data.

Keywords: Equation Learning, Stochastic Dynamics, Data-Driven Model Discovery, Langevin Dynamics, Stochastic Differential Equation

I. INTRODUCTION

In modelling complex dynamical systems, we often begin with a simple set of rules or processes at fine (local) scales. For example, in the context of ecological populations, this could be birth or death of individuals [1], interactions between organisms [2] and environment [3, 4], group and individual movement [5–7], etc. We then proceed to derive how these local interactions scale to the level of the groups, populations or even ecosystems [4, 7–10]. For analytically tractable systems, these coarse scale dynamical descriptions are often in the form of differential equations (ordinary, stochastic or even partial) [11].

We are now in the era of big data, where gathering high-resolution data capturing dynamics of biological systems is increasingly becoming common [12, 13]. Examples include, but are not limited to, population sizes [14, 15], fitness of population [16], ecosystem states observed via satellite derived indices [17, 18], how animals move [13], or how group properties evolve as a

function of time [5, 19, 20]. In systems such as schooling fish or microbial populations, the temporal resolution can be remarkably high. In many of these systems, the dynamics are subject to stochastic effects. The stochastic nature may arise due to inherent stochasticity in individual behaviour [19], demographic noise [4], or unobserved degrees of freedom whose effect on the observed time-series can be approximated as state-dependent stochastic forcing [21]. Such stochasticity can often produce counter-intuitive effects that are absent in the purely deterministic systems modelled by ordinary differential equations [22]. Therefore, in an era of data-driven modelling, a central question is the following: is it possible to construct dynamical models, accounting for both deterministic and stochastic effects, starting from observed time series data?

Indeed, the answer is in the affirmative. On one hand, methods from the traditional approaches to stochastic calculus allow us to infer stochastic differential equations from time-series data [21, 23–26]; more specifically, given the temporal evolution of a state variable x , one can construct the governing dynamical equation that via a stochastic differential equation (SDE) of the form $dx/dt = f(x) + g(x)\eta(t)$ (interpreted in an *Ito sense*);

* These authors contributed equally to the manuscript.

where $f(x)$ is the deterministic or drift function, $g^2(x)$ is the stochastic or diffusion function and $\eta(t)$ is a Gaussian white noise [27]. On the other hand, equation learning techniques [28, 29] have been recently developed, which can directly extract governing equations from observed data. More recently, several studies [30–32] have sought to combine these two approaches to directly extract SDEs from data. Combining equation learning with the traditional methods of jump moments is powerful, since it allows us to extract parsimonious and interpretable SDE models directly from data.

In this manuscript, we provide **PyDaddy** (Python library for **Data Driven Dynamics**), a comprehensive and easy-to-use Python package for obtaining data-derived stochastic differential equations from time series data. The package takes a time series of state variables (denoted by x) as the input, and outputs an SDE. In addition to extracting the differential equation from the data, package also implements a variety of visualization and diagnostic utilities. We demonstrate the workflow with the help of a real dataset from collective animal motion literature [19], and provide a detailed documentation along with ready-to-use Python notebooks and a number of example datasets, to make the process of using the package easy.

II. BASIC THEORY OF DISCOVERING SDE MODELS FROM TIME-SERIES DATA

Given a time-series of some observed variable x , we wish to discover a stochastic differential equation of the form,

$$\dot{x} = f(x) + g(x)\eta(t) \quad (1)$$

that describes the time-dynamics of x . Here, f and g are functions of x , and $\eta(t)$ is δ -correlated white-noise (i.e. $\langle \eta(t)\eta(t') \rangle = \delta(t - t')$) [27]. Our goal is to reconstruct f and g using the observations of x .

PyDaddy combines traditional techniques for reconstructing the drift and diffusion components [24] with recently developed techniques for equation learning [28] to recover the functional forms of f and g . This is a two step process:

1. First, the drift and diffusion components, corresponding to f and g^2 are extracted from the time-series data using conditional moments. (see Section II A).
2. Next, the estimated drift and diffusion are used to fit functional forms for f and g^2 using sparse-regression (see Section II B).

The approach naturally extends to a vectoral time series as well. For example, for a two-dimensional $\mathbf{x} = \begin{bmatrix} x_1 \\ x_2 \end{bmatrix}$, the stochastic differential equation takes the form

$$\dot{\mathbf{x}} = \mathbf{f}(\mathbf{x}) + \mathbf{g}(\mathbf{x}) \cdot \boldsymbol{\eta} \quad (2)$$

Here,

$$\mathbf{f}(\mathbf{x}) = \begin{bmatrix} f_1(x_1, x_2) \\ f_2(x_1, x_2) \end{bmatrix} \quad \text{and}$$

$$\mathbf{g}(\mathbf{x}) = \begin{bmatrix} g_{11}(x_1, x_2) & g_{12}(x_1, x_2) \\ g_{21}(x_1, x_2) & g_{22}(x_1, x_2) \end{bmatrix}$$

are the deterministic and the stochastic components respectively. $\boldsymbol{\eta} = \begin{bmatrix} \eta_1 \\ \eta_2 \end{bmatrix}$ is the uncorrelated Gaussian white noise vector. In many cases of interest, we will have $g_{12} = g_{21} = 0$, i.e. the cross stochastic terms vanish or are negligible. When the cross-terms are present, the estimation and interpretation of the diffusion becomes tricky—see Appendix A for more details.

A. Estimating drift and diffusion coefficients

We begin with a review of the conventional Kramers-Moyal averaging approach for estimating the drift and diffusion coefficients. In theory, the drift and diffusion components can be extracted from the time-series data in terms of the following ensemble averages[5, 33, 34]:

$$f(\tilde{x}) = \lim_{\Delta t \rightarrow 0} \left\langle \frac{x(t + \Delta t) - x(t)}{\Delta t} \middle| x(t) = \tilde{x} \right\rangle \quad (3)$$

$$g^2(\tilde{x}) = \lim_{\delta t \rightarrow 0} \left\langle \frac{(x(t + \delta t) - x(t))^2}{\delta t} \middle| x(t) = \tilde{x} \right\rangle \quad (4)$$

In practice, we only have access to a finite number of data-points of $x(t)$, sampled at some finite sampling interval. Therefore, the $\Delta t, \delta t \rightarrow 0$ limits are replaced by the finite-differences, and the ensemble average is typically replaced by a bin-wise average.

$$F(\tilde{x}) = \left\langle \frac{x(t + \Delta t) - x(t)}{\Delta t} \middle| \tilde{x} \leq x(t) < \tilde{x} + \epsilon \right\rangle \quad (5)$$

$$G(\tilde{x}) = \left\langle \frac{(x(t + \delta t) - x(t))^2}{\delta t} \middle| \tilde{x} \leq x(t) < \tilde{x} + \epsilon \right\rangle \quad (6)$$

The estimated drift function F is direct estimate for f , in both scalar and vector cases. The estimated diffusion function G is an estimate of g^2 in the scalar case, and an estimate for $\mathbf{g}\mathbf{g}^\top$ in the vector case.

When combined with sparse-regression-based equation-learning, the bin-wise averaging mentioned above becomes superfluous (see Section II B).

1. Assumptions underlying the Kramers-Moyal approach

The above approach works when the generating process for the time-series can be well-approximated by a drift-diffusion SDE. In particular, the following assumptions need to hold for the estimation to be accurate [24, 34]:

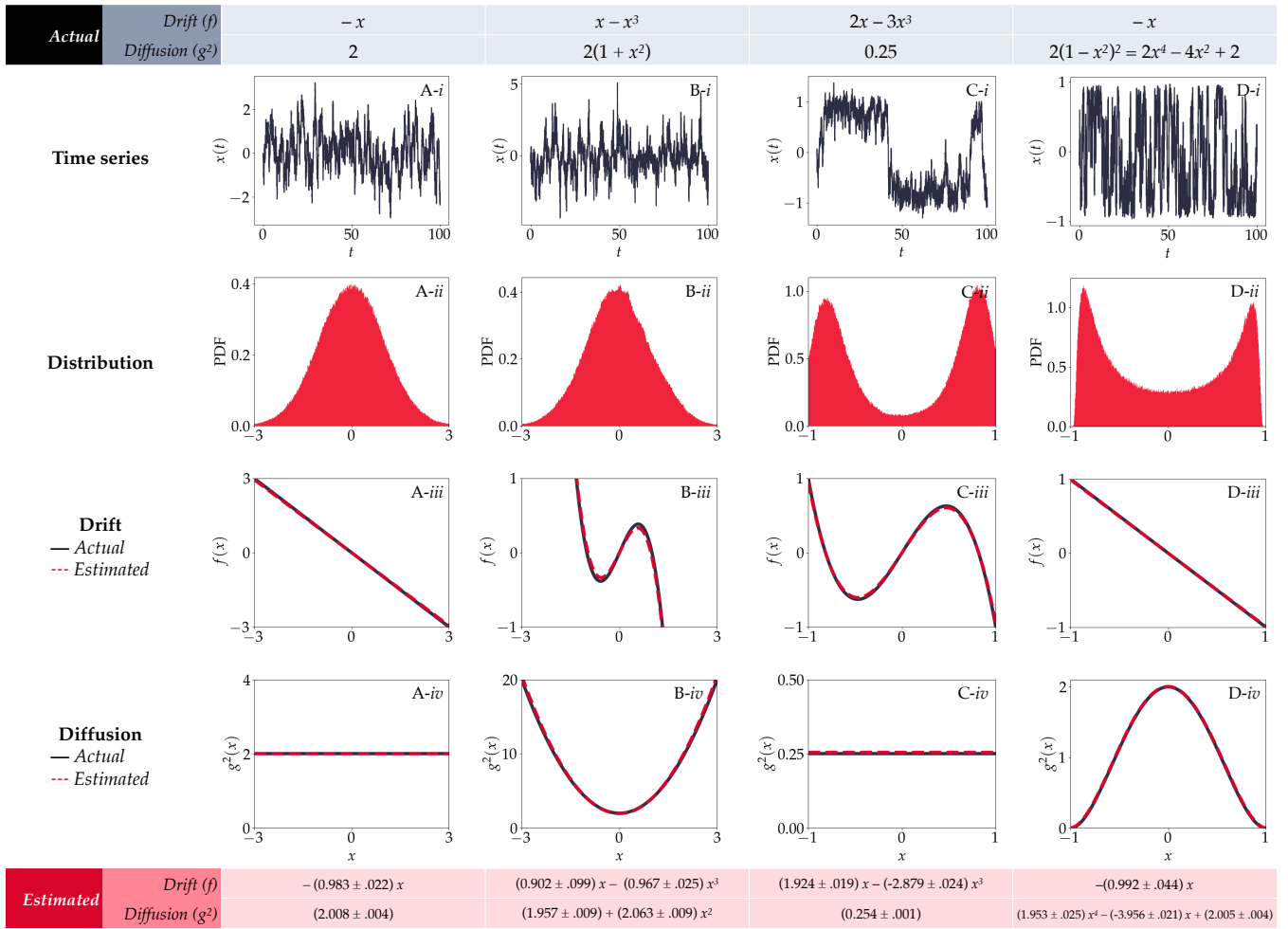


FIG. 1. **PyDaddy reliably reconstructs governing equations from simulated SDE data, for a wide range of dynamics.** Row i shows a sample of the time-series $x(t)$, and row ii shows the histogram of $x(t)$. Rows iii and iv show the actual (black) and estimated (red dashed) drift and diffusion functions. (A) A simple Ornstein-Uhlenbeck process, with a linear drift and constant diffusion, giving rise to a unimodal probability distribution of $x(t)$. (B) A system with a cubic drift and a quadratic diffusion function, also giving rise to a unimodal probability distribution of $x(t)$. PyDaddy is able to distinguish between these two systems, despite the steady-state distributions looking similar. (C) A bistable system with cubic drift and constant diffusion, with two stable states, giving rise to a bimodal probability distribution. The bimodality here is deterministic. (D) A bistable system with a linear drift and a quadratic diffusion, also with two stable states, giving rise to a bimodal probability distribution. The bimodality here is noise-induced. In all the cases, PyDaddy estimated functions closely match the actual functions.

- The residuals, defined as $r(t) = \dot{x}(t) - F(x(t))$, should be normally distributed. For vector time-series, the residuals should also be isotropic, i.e. the x - and y -components of the residuals should be uncorrelated.
- The residuals should be uncorrelated across time.
- *Pawula's Theorem*: Similar to the drift and diffusion components, one can also estimate higher moments from the data. Pawula's theorem states that, for a drift-diffusion SDE, the third and higher moments should be zero [27].

In practical scenarios, where we have a finite time-series sampled at a finite sampling time, the estimated

higher moments will not go to zero in general. In this case, alternative to Pawula theorem would be that $K_4(x) \approx 3 \cdot K_2(x)^2$, where K_2 and K_4 are the second and fourth Kramers-Moyal moments respectively. [24, 35]

B. Equation learning with sparse regression

Our goal is to find functional forms for the drift and diffusion functions f and g , based on the drift and diffusion coefficients estimated from the previous section. We use the approach of [28] for this—the key idea is to consider a (large) library of candidate *terms*, and use sparse regression to represent f or g as a linear combination of only a few terms from the library.

A crucial point to note is that the conditional averaging from equations 5 and 6 is not necessary for regression: data normally distributed around the ‘true’ value is sufficient.

Let $\mathbf{f}_{T \times 1}$ be the column vector consisting of the estimated drift coefficient at different points in time (T time-points in total), i.e

$$\mathbf{f} = \left[\frac{x(t + \Delta t) - x(t)}{\Delta t} \right]_{x=0, \Delta t, 2\Delta t, \dots} \quad (7)$$

Let $\mathfrak{F} = \{f_1 \dots f_k\}$ be the set of candidate terms, and let $\Theta_{T \times k}$ be a matrix where each column $\theta_j = f_j(x)$, $\mathbf{x}_{T \times 1}$ being the observed time-series x as a column-vector. We need to find a sparse vector $\boldsymbol{\xi}$ such that

$$\mathbf{f} = \Theta \boldsymbol{\xi} \quad (8)$$

There are several sparse regression techniques that allow us to find such a sparse $\boldsymbol{\xi}$: a technique that works particularly well in this scenario is called *sequentially thresholded least-squares* (STLSQ), which works as follows: first, $\boldsymbol{\xi}$ is fit using usual least-squares regression. Then, for an appropriate threshold ν , all entries in $\boldsymbol{\xi}$ which are less than ν are set to 0, and the corresponding columns of Θ are deleted. The least-squares regression fit is then repeated with the remaining columns. The process is repeated until all remaining terms in $\boldsymbol{\xi}$ are greater than ν .

The library Θ should ideally be chosen appropriately according to the problem in consideration. By default, PyDaddy uses polynomial terms upto a specified degree, but permits the user to specify a custom library if required.

C. Recovering SDEs from synthetic datasets

To benchmark the estimation performance of PyDaddy, we evaluated our method on several simulated systems, where the ground-truth governing dynamics are known. We generated simulated stochastic time-series from SDEs, using several different choices of f and g . We then used PyDaddy to estimate $f(x)$ and $g(x)$ from the simulated time-series. The following models were used in the analysis:

$$f(x) = -x, \quad g(x) = \sqrt{2} \quad (9)$$

$$f(x) = x - x^3, \quad g(x) = 2\sqrt{1+x^2} \quad (10)$$

$$f(x) = 2x - 3x^3, \quad g(x) = \frac{1}{2} \quad (11)$$

$$f(x) = -x, \quad g(x) = \sqrt{2}(1-x^2) \quad (12)$$

The functions were chosen such that equations 9 and 10 generate time series with identical, unimodal steady-state distributions. Similarly, equations 11 and 12 give

rise to similar bimodal distributions. However, the drift and diffusion functions—and consequently, the underlying dynamics—In 9, the single stable state is deterministic, with the additive noise simply spreading the dynamics around the stable state. On the other hand, in 10, the multiplicative noise-term completely alters the stability landscape, destroying the deterministic stable states at ± 1 and creating a new stable state at 0. Similarly, equations 11 and 12 give rise to similar bimodal distributions. In 11, the two stable states are deterministic, with the additive noise term $g(x)$ only causing a spread around the stable state. On the other hand, the deterministic term of 12 only has one stable state, the two stable states at ± 1 in this case are noise-induced.

Distinguishing between 9 and 10 (similarly 11 and 12) from observed data is challenging: one cannot rely on the steady-state distribution to identify the underlying model, the distinguishing features are only present in the temporal aspects of the dynamics. Nevertheless, PyDaddy is able to accurately identify the governing SDEs for each of the above examples. The drift functions recovered by PyDaddy match the actual equations almost exactly, illustrating the power of the approach.

III. PYDADDY: SDE ESTIMATION WORKFLOW

This section describes the organization of the PyDaddy package, and walks through a typical estimation workflow using a vector dataset. The dataset consists of average group polarization data for a school of fish [19]. The movement of a group of 15 *Etroplus suratensis* fish was recorded and their trajectories (i.e. positions and velocities at each instant of time) were tracked. From the trajectories of individual fish, the average group polarization vector \mathbf{m} (the mean of the normalized velocity vectors of the individual fish) was calculated at each instant of time. The final polarization time-series has a sampling interval of 0.12s.

The group polarization is a measure of how well aligned the school is at any point in time. Since the individual fish interact with each other and change direction stochastically, finite-size fish schools show stochastic fluctuations in the group polarization. Our goal is to use the school polarization dataset to extract an SDE that describes the dynamics of the group polarization.

A. Installation and documentation

The PyDaddy package is available on the PyPI repo, and can be installed using the following command:

```
pip install pydaddy
```

The package documentation is hosted at <https://pydaddy.readthedocs.io> and the full code is available at the GitHub repository <https://github.com/tee-lab/PyDaddy>.

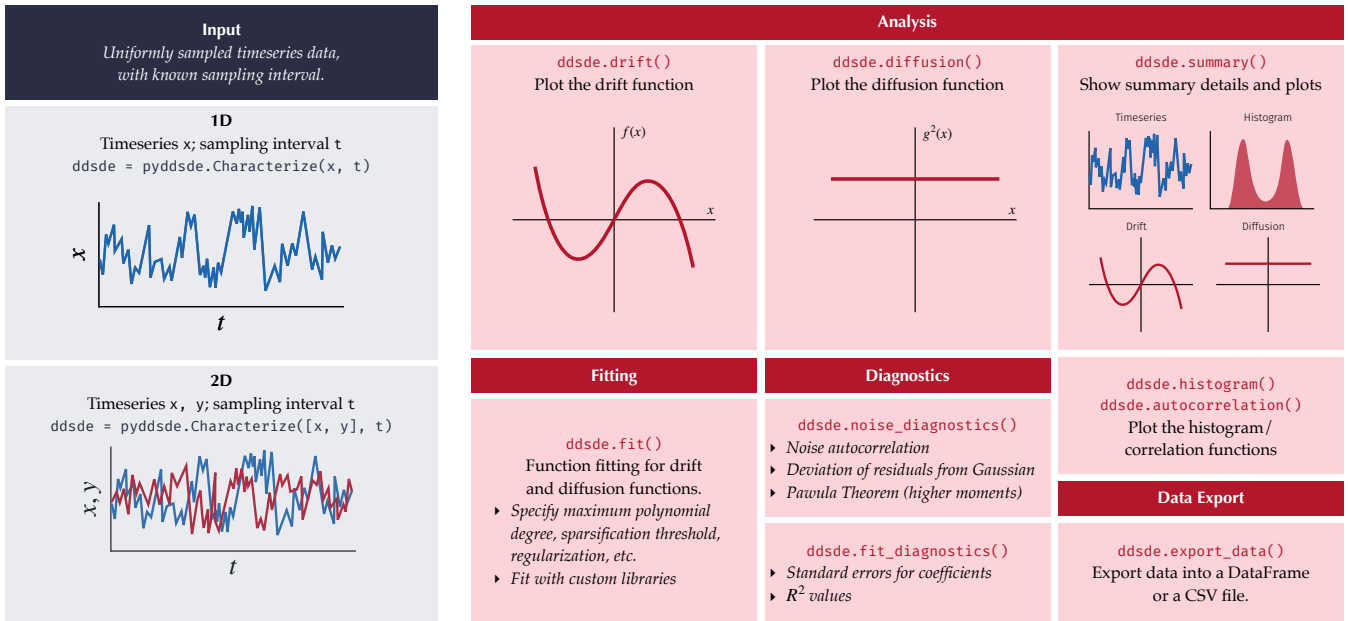


FIG. 2. **Overall schematics of the PyDaddy package.** PyDaddy takes as input uniformly sampled 1D or 2D time-series, and computes the drift and diffusion components from the time-series. Several functions are provided to visualize data as time-series or histograms, fit drift and diffusion functions, diagnose whether underlying assumptions for drift-diffusion estimation are met, and to export data.

B. Package organization

PyDaddy supports working with 1-D or 2-D time-series data. Timeseries should be regularly sampled with a known sampling interval. The package can compute, visualize, and fit drift and diffusion functions from provided timeseries. Diagnostic tools are provided to verify that assumptions necessary for modelling the timeseries as an SDE are met. Finally, PyDaddy can export data into a DataFrame or a CSV file—see Figure 2 for an overview of package capabilities.

C. Initialization and summary plot

The estimation workflow starts by creating a PyDaddy object.

```
dd = pydaddy.Characterize(data, t=0.1)
```

This creates a PyDaddy object called `dd`, estimates the drift and diffusion functions from the given time-series data, and shows a summary figure (Figure 3). The summary figure shows a sample of the timeseries, the autocorrelation functions, and histograms of the data. In addition, the estimated drift and diffusion functions are also shown. Functions—namely, `histogram()`, `autocorrelation()`, `drift()`, `diffusion()` and `cross_diffusion()`—are provided to explore each of these features in detail.

The drift and diffusion plots, shown in the summary as well as available using the functions `drift()`, `diffusion()` and `cross_diffusion()`, show the estimated shapes of the drift and diffusion functions respectively. These plots can be used to identify qualitative features of the dynamics, such as the nature and positions of the deterministic equilibrium points, nature of the state-dependent noise (i.e. diffusion), presence or absence of cross diffusion, etc.

D. Diagnostics

Before proceeding further, it is essential to ensure that the assumptions involved in modelling the time-series as an SDE (Section II A 1) are not violated. PyDaddy provides diagnostic functions to verify that the assumptions are met. Diagnostic plots in PyDaddy can be generated using

```
dd.noise_diagnostics()
```

Figure 4 shows the diagnostic plots produced by PyDaddy. The diagnostic plots show the following:

- The distribution of the residuals—the residuals should be normally distributed around 0. For vector time-series, the correlation matrix is shown as an inset: this should be the 2×2 identity matrix.
- Autocorrelation of the residual timeseries—the autocorrelation time should be close to 0 (and

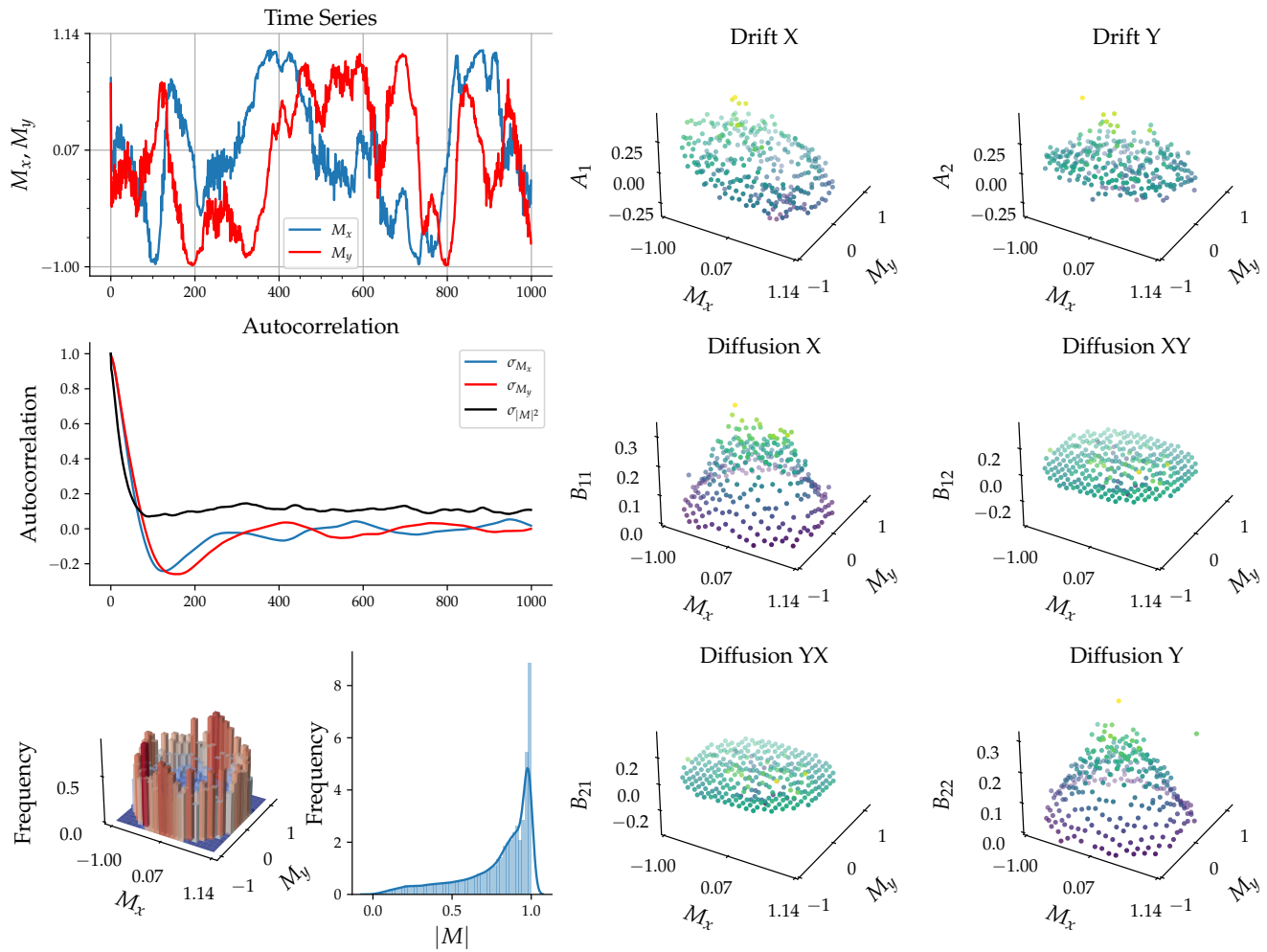


FIG. 3. **The summary plot generated by PyDaddy.** The plot was generated by PyDaddy by processing the fish school polarization timeseries (vector data). The left half of the plot shows the time-series, autocorrelation functions, histograms of the provided data. The right half shows the estimated drift and diffusion coefficients, estimated using binwise-averaged jump moments.

much smaller than one time-step). For vector time-series, the autocorrelation of both marginals η_x and η_y , as well as that of $|\eta|^2 = \eta_x^2 + \eta_y^2$ are shown.

- QQ plots of the residuals against a theoretical Gaussian distribution—the points should lie on a straight line of unit slope. For vector time-series, QQ plots of the marginal distributions are shown.
- The plot of the second and fourth Kramers-Moyal coefficients, specifically $3 \cdot K_2^2$ against K_4 . The points should lie along the straight line of unit slope.

E. Fitting drift and diffusion functions

The drift and diffusion plots from above give a qualitative picture of the dynamics of the system. PyDaddy can go a step beyond and fit actual functional forms for

the drift and diffusion functions. To do this, use the `fit()` function of the `dd` object.

As mentioned in Section II B, fitting is done using sparse regression, and by default fits polynomial functions of a specified degree. The sparsification threshold, which governs the number of terms in the fit (see Section II B can be either chosen automatically using cross-validation (see Appendix B), or be set manually.

For example,

```
dd.fit('A1', order=3, tune=True, plot=True)
```

fits a degree-3 polynomial with sparsification threshold chosen automatically. The first argument names the function to be fitted: `A1` and `A2` correspond to the two components of the drift; `B11` and `B22` correspond to diffusion, and `B12` and `B21` correspond to cross diffusion. The `plot=True` argument tells the function to produce a cross-validation error plot for a range of thresholds

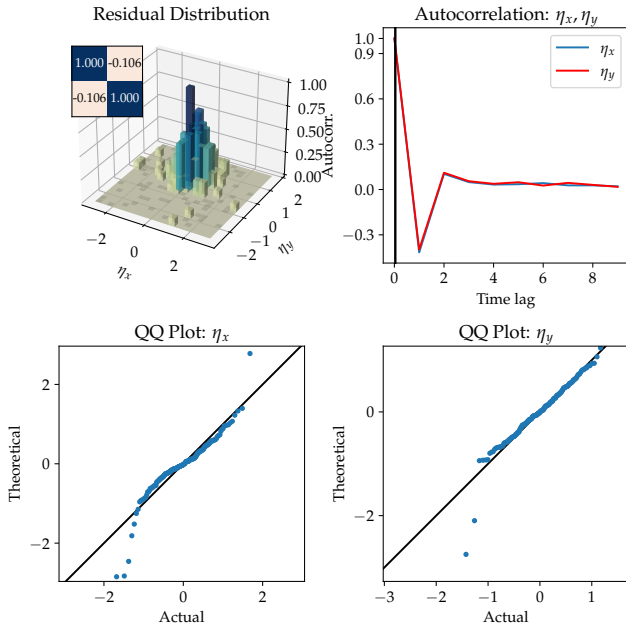


FIG. 4. **Diagnostic figures generated by PyDaddy.** The first panel shows the distribution of the residuals, which should ideally be a Gaussian. The second panel shows the autocorrelation functions, with the black line marking the autocorrelation time: ideally, the autocorrelation time should be $\ll 1$. The third and fourth panels show the QQ-plots of the marginal distributions, which should ideally fall on a line of slope 1.

(see Figure 5). The ideal threshold should strike a balance between the error and number of terms in this plot. PyDaddy chooses as high as a threshold as possible without increasing the cross-validation error too much—see Appendix B for details.

The sparsification threshold can be interpreted as follows: for a given value of sparsification threshold, all the coefficients in the returned polynomial will be above this threshold. This intuition can be used to manually optimize the threshold to eliminate terms. For example,

```
dd.fit('A1', order=3, threshold=0.1)
```

produces a polynomial with degree upto 3, with only terms with coefficient 0.1 or higher.

Figure 6 shows the drift and diffusion functions estimated by PyDaddy for the example timeseries. In line with previous results [19], we find a linear drift and a quadratic diffusion, suggesting that the group polarization is noise-induced. The cross-diffusion terms (not shown) were negligible and were fit by the zero polynomial.

In the drift and diffusion functions in Figure 6, coefficients with overlapping error-bars can be combined (by replacing them with their averages), to get the following vector SDE:

$$\dot{\mathbf{m}} = -0.147\mathbf{m} + \sqrt{0.021 + 0.236(1 - |\mathbf{m}|^2)} \cdot \boldsymbol{\eta}(t) \quad (13)$$

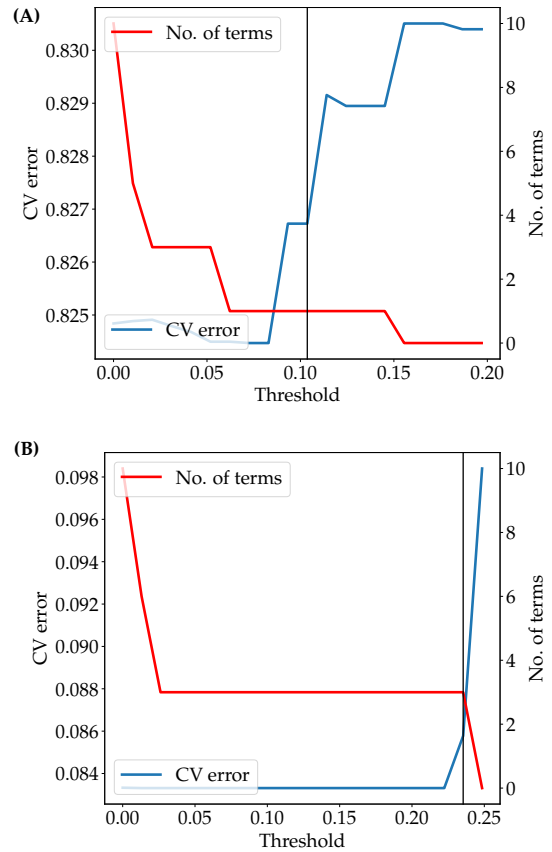


FIG. 5. **PyDaddy model selection.** PyDaddy uses cross validation to choose the correct level of sparsification. (A) The cross-validation error and the number of selected terms at each level of sparsity, while fitting the drift function A_1 . The black line shows the threshold chosen by the cross validation algorithm, which produces a polynomial with just 1 term. (B) Similar plot for fitting the diffusion function B_{11} . The chosen threshold here corresponds to a polynomial with 3 terms.

An important point to note: although PyDaddy provides functionality for automatic model selection, model selection, model selection works best when coupled with some human input based on theory and understanding of the system. In particular, the order of the polynomial needs to be specified based on visual inspection of the drift/diffusion plots or using theoretical understanding. The PyDaddy documentation [36] contains an extended discussion about this aspect.

IV. DISCUSSION

Here, we have presented a python package pyDaddy—an easy-to-use tool for data-driven discovery of dynamics of complex systems: specifically, PyDaddy seeks to find a data-driven stochastic differential equation that captures the dynamics of the observed state variable. We combined the traditional approaches

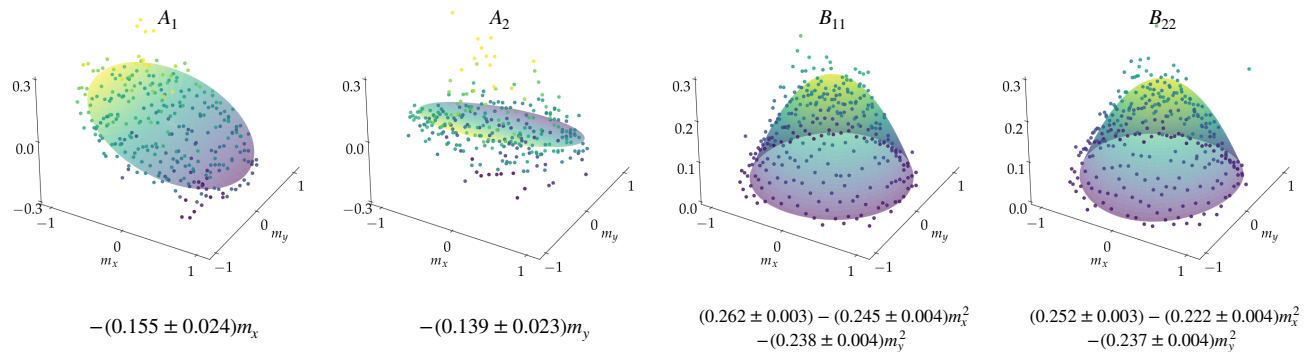


FIG. 6. **The drift and diffusion functions estimated by PyDaddy.** The estimated drift and diffusion functions are plotted alongside the binwise averaged jump moments. A_1 and A_2 are the components of the drift function, and B_{11} and B_{22} are the components of the diffusion function. The estimated polynomials returned by PyDaddy are shown below each of the plots.

of drift and diffusion estimation using jump moments, with equation-discovery techniques based on sparse regression to recover SDE models from time-series data. Importantly, the use of sparse regression helped us eliminate certain arbitrary choices of parameters (such as bin-size and subsampling time) used in previous methods [25, 26]. Equally importantly, we provide visual and diagnostic tools to test the assumptions associated with data-derived functions, sparse fits, as well as the noise.

We demonstrated the method with a time series data of schooling fish. However, it is readily applicable to any ecological system, or more generally any dynamical system, where sufficiently highly resolved and long data are available. This raises the obvious question: how finely resolved and how long a time series is necessary? As demonstrated in previous studies [25], the time series must be at around an order of magnitude (or more) finely resolved than the autocorrelation time of the state variable. When the time resolution is comparable or more than the autocorrelation time, the dynamics of the system can't be captured; for such coarse time series, the estimated drift and diffusion functions typically converge to a linear and upward-parabolic functions, independent of the actual dynamics [26]. While we are not aware of any studies that have looked at the minimum length required to estimate the drift and diffusion reliably, based on our own numerical simulations of models shown in this study, we speculate that the total length must be at least a few orders of magnitude times the length of the autocorrelation time.

While such datasets may not be abundant right now, we are indeed making rapid headways towards collecting such data in many ecological systems. At the scale of individual organisms, both tag-based (radio collar, GPS, etc) and high-resolution video based tracking of animals [37] (or cells [38]) yield high spatio-temporal resolution data of how animals (or cells) move in space. At the level of groups, we have already demonstrated the example of collective motion of fish, where such data are now increasingly available for many organisms,

from collective cell migration [39] to insect swarms to flocking birds [40]. Finally, long time series are becoming available for populations (especially microbial) and even ecosystems [41, 42]; for example, sensors that capture water quality at high resolution [43] (e.g. every second) make characterisation of lake ecosystem states in a rigorous mathematical way. We expect that availability of such datasets will only become more abundant in the coming years, across scales of biological systems.

We also expect many challenges, and hence opportunities for future work, when applying these methods to complex ecological systems. First, despite the fact that we have automated various steps, there are still a few choices the user will make. These include the choice of the functions the user will chose to fit and the sparsity threshold, since a less sparse function (i.e. one with more terms) will always explain the variation of data better. We suggest that one must choose the best fit functions using the '*principle of parsimony*', and be guided by theory when possible. We have already alluded to the importance of length of time series, and how it may impact on what we find as best-fit functions. Secondly, in the current framework of SDEs, the structure of noise is Gaussian and uncorrelated. This could be too simplistic since many ecosystems are affected by different types of perturbations and stochasticity; for example, a single large natural or human induced calamity is better modelled as a shot noise rather than a Gaussian white noise [44]. Noise in real systems may also be temporally correlated [45]. Finally, the key drivers of the system may show seasonality (e.g. rainfall, nutrient flow), thus violating the assumption of stationarity which is necessary for discovering SDEs from time series data. Modifying and adopting the package described here to account for realistic features presents interesting directions for future work.

In summary, as the era of big data looms over much of biological sciences including ecology, we hope that our presentation of a (relatively) easy to use package that helps us characterise the governing dynamical equations from the data will inspire usage of these relatively

unknown methods in the field of ecology and more

broadly, to other complex dynamical systems.

-
- [1] A. J. McKane and T. J. Newman, Stochastic models in population biology and their deterministic analogs, *Physical Review E* **70**, 041902 (2004).
- [2] H. Cheng, N. Yao, Z.-G. Huang, J. Park, Y. Do, and Y.-C. Lai, Mesoscopic interactions and species coexistence in evolutionary game dynamics of cyclic competitions, *Scientific Reports* **4**, 1 (2014).
- [3] A. J. Black and A. J. McKane, Stochastic formulation of ecological models and their applications, *Trends in ecology & evolution* **27**, 337 (2012).
- [4] S. Majumder, A. Das, A. Kushal, S. Sankaran, and V. Guttal, Finite-size effects, demographic noise, and ecosystem dynamics, *The European Physical Journal Special Topics* **230**, 3389 (2021).
- [5] C. A. Yates, R. Erban, C. Escudero, I. D. Couzin, J. Buhl, I. G. Kevrekidis, P. K. Maini, and D. J. T. Sumpter, Inherent noise can facilitate coherence in collective swarm motion, *Proceedings of the National Academy of Sciences* **106**, 5464 (2009).
- [6] M. A. Lewis, P. K. Maini, and S. V. Petrovskii, Dispersal, individual movement and spatial ecology, *Lecture Notes in Mathematics (Mathematics Bioscience Series)* **2071** (2013).
- [7] J. Jhavar, R. G. Morris, and V. Guttal, Deriving Mesoscopic Models of Collective Behavior for Finite Populations, in *Handbook of Statistics*, Vol. 40 (Elsevier, 2019) pp. 551–594.
- [8] M. Loreau, From populations to ecosystems, in *From Populations to Ecosystems* (Princeton University Press, 2010).
- [9] R. Durrett and S. Levin, The importance of being discrete (and spatial), *Theoretical population biology* **46**, 363 (1994).
- [10] T. Biancalani, L. Dyson, and A. J. McKane, Noise-induced bistable states and their mean switching time in foraging colonies, *Physical review letters* **112**, 038101 (2014).
- [11] N. J. Gotelli *et al.*, *A primer of ecology*, Vol. 494 (Sinauer Associates Sunderland, MA, 2008).
- [12] S. Leyk, A. E. Gaughan, S. B. Adamo, A. de Sherbinin, D. Balk, S. Freire, A. Rose, F. R. Stevens, B. Blankespoor, C. Frye, *et al.*, The spatial allocation of population: a review of large-scale gridded population data products and their fitness for use, *Earth System Science Data* **11**, 1385 (2019).
- [13] R. Nathan, C. T. Monk, R. Arlinghaus, T. Adam, J. Alós, M. Assaf, H. Baktoft, C. E. Beardsworth, M. G. Bertram, A. I. Bijleveld, *et al.*, Big-data approaches lead to an increased understanding of the ecology of animal movement, *Science* **375**, eabg1780 (2022).
- [14] N. C. Stenseth, W. Falck, O. N. Bjørnstad, and C. J. Krebs, Population regulation in snowshoe hare and canadian lynx: asymmetric food web configurations between hare and lynx, *Proceedings of the National Academy of Sciences* **94**, 5147 (1997).
- [15] O. N. Bjørnstad and B. T. Grenfell, Noisy clockwork: time series analysis of population fluctuations in animals, *Science* **293**, 638 (2001).
- [16] R. E. Lenski, Experimental evolution and the dynamics of adaptation and genome evolution in microbial populations, *The ISME journal* **11**, 2181 (2017).
- [17] Y. Xie, Z. Sha, and M. Yu, Remote sensing imagery in vegetation mapping: a review, *Journal of plant ecology* **1**, 9 (2008).
- [18] S. Majumder, K. Tamma, S. Ramaswamy, and V. Guttal, Inferring critical thresholds of ecosystem transitions from spatial data, *Ecology* **100**, e02722 (2019).
- [19] J. Jhavar, R. G. Morris, U. Amith-Kumar, M. Danny Raj, T. Rogers, H. Rajendran, and V. Guttal, Noise-induced schooling of fish, *Nature Physics* **16**, 488 (2020).
- [20] K. Tunstrøm, Y. Katz, C. C. Ioannou, C. Huepe, M. J. Lutz, and I. D. Couzin, Collective states, multistability and transitional behavior in schooling fish, *PLoS computational biology* **9**, e1002915 (2013).
- [21] R. Friedrich, J. Peinke, M. Sahimi, and M. R. R. Tabar, Approaching complexity by stochastic methods: From biological systems to turbulence, *Physics Reports* **506**, 87 (2011).
- [22] W. Horsthemke and R. Lefever, Noise-induced transitions, *Noise in nonlinear dynamical systems* **2**, 179 (1989).
- [23] J. Gradišek, S. Siegert, R. Friedrich, and I. Grabec, Analysis of time series from stochastic processes, *Physical Review E* **62**, 3146 (2000).
- [24] R. Tabar, *Analysis and data-based reconstruction of complex nonlinear dynamical systems*, Vol. 730 (Springer, 2019).
- [25] J. Jhavar and V. Guttal, Noise-induced effects in collective dynamics and inferring local interactions from data, *Philosophical Transactions of the Royal Society B* **375**, 20190381 (2020).
- [26] R. Philip, G. Lind Pedro, W. Matthias, and P. Joachim, The langevin approach: An r package for modeling markov processes, *Journal of Open Research Software* **4** (2016).
- [27] C. Gardiner, *Stochastic methods*, Vol. 4 (springer Berlin, 2009).
- [28] S. L. Brunton, J. L. Proctor, and J. N. Kutz, Discovering governing equations from data by sparse identification of nonlinear dynamical systems, *Proceedings of the national academy of sciences* **113**, 3932 (2016).
- [29] S. H. Rudy, S. L. Brunton, J. L. Proctor, and J. N. Kutz, Data-driven discovery of partial differential equations, *Science advances* **3**, e1602614 (2017).
- [30] L. Boninsegna, F. Nüske, and C. Clementi, Sparse learning of stochastic dynamic equations, *The Journal of Chemical Physics* **148**, 241723 (2018), arXiv: 1712.02432.
- [31] J. L. Callahan, J.-C. Loiseau, G. Rigas, and S. L. Brunton, Nonlinear stochastic modelling with langevin regression, *Proceedings of the Royal Society A* **477**, 20210092 (2021).
- [32] Y. Huang, Y. Mabrouk, G. Gompper, and B. Sabass, Sparse inference and active learning of stochastic differential equations from data, arXiv preprint arXiv:2203.11010 (2022).
- [33] N. G. Van Kampen, *Stochastic processes in physics and chemistry*, Vol. 1 (Elsevier, 1992).
- [34] A. Kolpas, J. Moehlis, and I. G. Kevrekidis, Coarse-grained analysis of stochasticity-induced switching between collective motion states, *Proceedings of the National Academy of Sciences* **104**, 5931 (2007).
- [35] K. Lehnertz, L. Zabawa, and M. R. R. Tabar, Characterizing abrupt transitions in stochastic dynamics, *New Journal of Physics* **20**, 113043 (2018).

- [36] Pydaddy tutorials – advanced function fitting, https://pydaddy.readthedocs.io/en/latest/tutorials/3/advanced_fitting.html (2022), [Online; accessed 1-May-2022].
- [37] R. Kays, M. C. Crofoot, W. Jetz, and M. Wikelski, Terrestrial animal tracking as an eye on life and planet, *Science* **348**, aaa2478 (2015).
- [38] O. Hilsenbeck, M. Schwarzfischer, S. Skylaki, B. Schauburger, P. S. Hoppe, D. Loeffler, K. D. Kokkaliaris, S. Hastreiter, E. Skylaki, A. Filipczyk, *et al.*, Software tools for single-cell tracking and quantification of cellular and molecular properties, *Nature biotechnology* **34**, 703 (2016).
- [39] M. Poujade, E. Grasland-Mongrain, A. Hertzog, J. Jouanneau, P. Chavrier, B. Ladoux, A. Buguin, and P. Silberzan, Collective migration of an epithelial monolayer in response to a model wound, *Proceedings of the National Academy of Sciences* **104**, 15988 (2007).
- [40] A. Cavagna, S. D. Queirós, I. Giardina, F. Stefanini, and M. Viale, Diffusion of individual birds in starling flocks, *Proceedings of the Royal Society B: Biological Sciences* **280**, 20122484 (2013).
- [41] P. Trosvik, K. Rudi, T. Næs, A. Kohler, K.-S. Chan, K. S. Jakobsen, and N. C. Stenseth, Characterizing mixed microbial population dynamics using time-series analysis, *The ISME journal* **2**, 707 (2008).
- [42] D. M. Karl and M. J. Church, Microbial oceanography and the hawaii ocean time-series programme, *Nature Reviews Microbiology* **12**, 699 (2014).
- [43] A. U. Alam, D. Clyne, and M. J. Deen, A low-cost multi-parameter water quality monitoring system, *Sensors* **21**, 3775 (2021).
- [44] K. L. Drury, Shot noise perturbations and mean first passage times between stable states, *Theoretical Population Biology* **72**, 153 (2007).
- [45] K. Johst and C. Wissel, Extinction risk in a temporally correlated fluctuating environment, *Theoretical Population Biology* **52**, 91 (1997).

Appendix A: Estimating diffusion with non-zero cross-diffusion terms

Consider the drift and diffusion estimation for a 2D vector dataset. Denote the estimated drift and diffusion functions as $A = \begin{bmatrix} A_1 \\ A_2 \end{bmatrix}$ and $B = \begin{bmatrix} B_{11} & B_{12} \\ B_{21} & B_{22} \end{bmatrix}$ respectively. As mentioned in Section II A, B corresponds to gg^\top where g is the stochastic component. That is,

$$\begin{bmatrix} B_{11} & B_{12} \\ B_{21} & B_{22} \end{bmatrix} = \begin{bmatrix} g_{11}^2 + g_{12}^2 & g_{11}g_{21} + g_{12}g_{22} \\ g_{11}g_{21} + g_{12}g_{22} & g_{21}^2 + g_{22}^2 \end{bmatrix} \quad (\text{A1})$$

This means that, when g_{12} or g_{21} is non-zero, the estimated diffusion coefficients B_{11} and B_{22} are combinations of straight and cross diffusion terms. Identifying g_{11} and g_{22} uniquely is not possible in this scenario—see [7] for further discussion of this issue.

Appendix B: Model selection for sparse regression

The sparsity threshold in the STLSQ procedure of Section II B is an operational parameter that needs to be chosen appropriately to ensure that the right models are recovered. For different values of the sparsity threshold, we will get different models, and we need to use some criterion to choose the threshold that produces the best model. One approach is to use an appropriate information criterion, like Akaike Information Criterion (AIC): the model for which the information criterion in minimum is the one that achieves the best trade-off between model fit and model complexity.

An alternate approach, popular in machine learning literature, is to choose the ideal model based on cross-validated accuracy. We chose this approach, and used *k-fold cross validation* for model selection, which we briefly describe here.

The key idea behind cross-validation is that a model that performs well on a held-out validation set will not have overfit on the noise in the training data, and may be more generalizable. The dataset is divided into k equal chunks. $k - 1$ of the chunks are used as the *training set* to fit the model, with the remaining chunk designated as the *validation set*. The validation set is used to compute the validation error for the fit model. The process is repeated with each of the k chunk designated as the validation set, and the average validation error is computed. The model that gives the minimum cross-validation error is chosen as the best model.

However, since model parsimony is crucial in our application, the model with the minimum cross validation error may not always be the best choice, as non-sparse models may sometimes end up getting selected. To avoid this, we instead sort the models in increasing order of complexity, and choose the model that achieves the *maximum drop* in cross-validation error from the previous model.